

ARTICLES

Photodissociation Dynamics of Iodoform in Solution

Magnus Wall, Alexander N. Tarnovsky, Torbjörn Pascher, Villy Sundström, and Eva Åkesson*

Department of Chemical Physics, Lund University, Box 124, S-22100 Lund, Sweden

Received: June 11, 2002; In Final Form: September 18, 2002

The photodissociation dynamics of iodoform (CHI_3) in acetonitrile and cyclohexane were investigated by femtosecond pump-probe spectroscopy and nanosecond laser flash photolysis. We have measured transient absorption spectra in the spectral region of 370–730 nm and kinetics at selected wavelengths on a femtosecond–microsecond time scale. We assign the observed photoproduct with absorption maxima at 450 and 600 nm, formed upon excitation of iodoform at 350 nm in acetonitrile and cyclohexane, to the isomer of iodoform, iso-iodoform ($\text{CHI}_2\text{-I}$). The iso-iodoform is most probably formed via an in-cage recombination of the produced photofragments, the I atom and the CHI_2 radical, with an ~ 7 ps time constant. The lifetime of the iso-iodoform is found to be ~ 1.8 and $0.2 \mu\text{s}$ in cyclohexane and acetonitrile, respectively.

I. Introduction

Photodissociation dynamics in solution are not as well characterized as those in the gas phase. In solution, photodissociation dynamics are influenced by solute–solvent interactions, and processes such as geminate recombination of the produced photofragments within the solvent cage can occur. For molecules with more than two atoms, the photofragments can recombine within the solvent cage into a configuration different from that of the parent molecule, that is, an isomer configuration. We have previously found that the dihalomethanes, CH_2I_2 , CH_2BrI , and CH_2ClI , form the $\text{CH}_2\text{I-I}$, $\text{CH}_2\text{Br-I}$, and $\text{CH}_2\text{Cl-I}$ isomers within the solvent cage on an $\sim 5\text{--}9$ ps time scale, upon excitation of their lower-lying states. In this study, we focus our interest on the polyhalomethane iodoform (CHI_3) to investigate whether in-cage isomerization also occurs for this group of molecules.

The measured ultraviolet (UV) absorption spectra of iodoform in cyclohexane and in acetonitrile are presented in Figure 1 and exhibit three broad bands in the spectral region of 250–400 nm and an intense absorption at wavelengths below 250 nm.

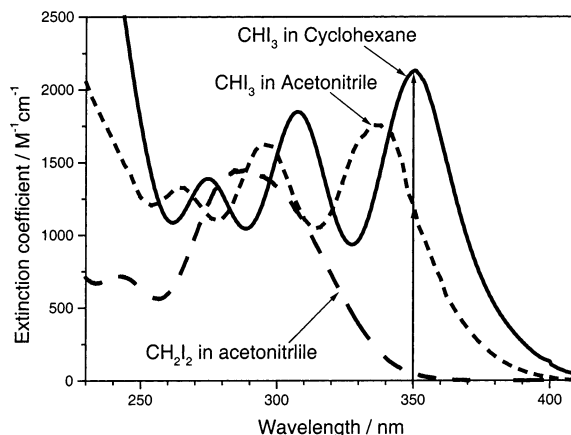


Figure 1. Absorption spectra of iodoform (CHI_3) in acetonitrile and cyclohexane, together with the absorption spectrum of diiodomethane (CHI_2) in acetonitrile. The vertical arrow indicates the excitation wavelength of 350 nm in the femtosecond experiments.

The arrow in Figure 1 indicates the excitation wavelength of 350 nm utilized in the femtosecond experiments. For comparison, the spectrum of diiodomethane (CH_2I_2) in acetonitrile is also shown. The spectral properties of iodoform are not as well

* To whom correspondence should be addressed. E-mail: Eva.akesson@chemphys.lu.se.

characterized as those for the closely related compounds CH_2I_2 and CH_3I . Generally, the low-energy optical transitions in alkylhalides involve the promotion of a nonbonding electron localized on a p-orbital of the halogen to an antibonding σ^* -orbital of the C–X bond ($n(\text{X}) \rightarrow \sigma^*(\text{C}-\text{X})$ transition). It is known that the dissociation of CH_3I at 266 nm in the gas phase mainly produces a spin-orbit excited $\text{I}^*(^2\text{P}_{1/2})$ iodine atom and the CH_3 radical.¹ The absorption spectrum of diiodomethane (CH_2I_2) in acetonitrile has two broad absorption bands located at 245 and 290 nm (see Figure 1). CH_2I_2 is known to dissociate in the gas phase to give an iodine atom in the ground-state $\text{I}(^2\text{P}_{3/2})$ or spin-orbit excited-state $\text{I}^*(^2\text{P}_{1/2})$ when excited with a relatively low-energy UV photon (<5 eV).^{2–7} Molecular beam experiments showed that the dissociation of diiodomethane occurs on repulsive potentials on a time scale faster than a rotational period, ~ 10 ps.^{5,7} The spectrum of iodoform in cyclohexane has absorption maxima at 275, 310, and 350 nm. The spectrum of iodoform in acetonitrile exhibits a relatively large blueshift of 1200 cm^{-1} , and the bands are broader compared with the spectrum of iodoform in cyclohexane. These features are a result of differing solvent polarities. The solvent-induced blueshift is typical for $n(\text{I}) \rightarrow \sigma^*(\text{C}-\text{I})$ transitions when going from a nonpolar solvent to a polar solvent. Solvent-dipole interactions in a polar solvent result in a broadening of the absorption bands. In addition, the intense absorption peak at shorter wavelengths (<250 nm) is most likely due to Rydberg transitions on the iodine atom, $np(\text{I}) \rightarrow ns(\text{I})$.

There are a few experimental studies reported on UV photolysis of iodoform.^{5,8–10} Bersohn et al.⁵ investigated the dissociation of iodoform in a molecular beam (gas phase) by polarized ultraviolet light. They found that iodoform dissociates, when excited in the two low-lying states (at 350 and 310 nm), to give an iodine atom (I) and the CHI_2 radical on a time scale much faster than the rotational period of the parent molecule. Excitation of the lowest-lying state of iodoform in mesitylene solution (~ 350 nm) with 3 ns laser pump pulses was assigned to result in a formation of an iodine-mesitylene complex immediately after the laser pulse.⁸ Recent nanosecond transient resonance Raman experiments of iodoform in cyclohexane solution,⁹ performed by exciting iodoform at 309.1 or at 368.7 nm and probing at 416.0 and 435.9 nm, indicated that the isomer configuration of iodoform, iso-iodoform (CHI_2-I), was the observed photoproduct immediately after excitation (~ 0 ns). Experimental vibrational frequencies of the iso-iodoform CHI_2-I , the CHI_2 radical, and the CHI_3^+ radical cation were compared with those calculated by density functional theory (DFT).⁹ A good agreement was only found for the iso-iodoform, CHI_2-I . The assignment in ref 9 of the ~ 400 nm absorption band observed in pulse radiolysis of iodoform in 1,2-dichloroethane¹⁰ to the iso-iodoform is also consistent with the results of the DFT calculations. The iso-iodoform is believed⁹ to form in the same manner as isodiiodomethane ($\text{CH}_2\text{I}-\text{I}$) after photodissociation of diiodomethane (CH_2I_2) in acetonitrile solution.¹¹ Extensive femtosecond pump-probe experiments of CH_2I_2 in acetonitrile have shown that the initially produced photofragments, iodine atom and CH_2I radical, recombine within the solvent cage to form the isomer of CH_2I_2 , isodiiodomethane ($\text{CH}_2\text{I}-\text{I}$), ~ 5 ps after excitation at 266, 310, and 350 nm.^{11,12}

In the present work, we have studied the photodissociation and photoproduct formation of iodoform in solution on an extensive time scale, ranging from femtoseconds to microseconds. We show the photoproduct spectra upon 350-nm excitation of iodoform in solution on a femtosecond time scale, which to our knowledge never have been done before. We

present a reaction mechanism for the photoproduct formation and estimate the lifetime of the observed photoproduct. These experimental results will provide a useful guideline to evaluate the accuracy of advanced ab initio calculations with included spin-orbit coupling of the excited states of iodoform and iso-iodoform, which are in progress at our department.

II. Experimental Section

The photodissociation dynamics of iodoform in acetonitrile and cyclohexane were investigated by measuring transient absorption spectra and kinetics on both a femtosecond and a nanosecond time scale. The femtosecond pump-probe experiments were performed with a 1 kHz amplified Ti-sapphire laser system with an output of ~ 100 -fs (fwhm) pulses centered at 800 nm with a pulse energy of ~ 0.9 mJ. The 350-nm pump pulses were the second harmonic of 700-nm light generated in a 0.4 mm BBO type I crystal. The 700-nm light was the second harmonic of signal output of a TOPAS. A color filter before the BBO crystal reduced the 800-nm residual and the IR output. The 700-nm residual was minimized by four dichroic mirrors before interaction with the sample. A white light continuum in the spectral region of 360–750 nm was used as analyzing light, and it was generated by focusing a fraction of either the 800-nm output pulses or its second harmonic, which was generated in a KDP crystal, into a sapphire plate. The time zero was obtained by using the nonresonant pump-probe signal from pure solvent, as described in ref 13. An instrument response function of ~ 230 fs (fwhm) was estimated at several probe wavelengths by deconvolution to the instantaneous rise of the transient absorption signal. All measurements were performed using magic angle polarization; that is, the angle between the pump and probe polarizations was 54.7° to eliminate the contribution from rotational dynamics of the solute to the measured signal. The angle between pump and probe beams was $\sim 7^\circ$, and the pulses were focused by lenses with focal distances $f_{\text{pump}} = 150$ mm and $f_{\text{probe}} = 75$ mm. The pump pulse energy was ~ 1 μJ at the sample position. The sample was circulated through a 0.2-mm-thick Spectrasil quartz flow cell to ensure fresh sample at each laser shot. The detection scheme used has been described earlier.¹⁴ Briefly, the white light was divided into probe and reference beams. After passing the sample and a monochromator, the two beams were detected separately by either two photodiodes, when measuring kinetics, or two diode arrays, when measuring transient absorption spectra. Great care was taken to ensure that the overlap did not change when moving the optical delay line. The overlap geometry was optimized to minimize the nonresonant signal from the solvent and the front cell window. The transient absorption spectra were corrected for the chirp after the measurements to ensure true time zeros for the different spectral components of the white light. The nanosecond measurements were performed with a nanosecond laser flash photolysis setup. Briefly, the 355 nm pump pulses were obtained by tripling the output of a Nd:YAG laser. The pump energy was 0.5 mJ/pulse, and the beam had a diameter of ~ 2 mm. Probe light from a xenon arc lamp was focused to a ~ 1 -mm-diameter spot at the sample position. After interaction with the sample, the probe light was passed through two monochromators and detected by a photomultiplier tube (PMT). The time resolution of the system depends on several factors, for example, signal-to-noise ratio and pulse length (~ 5 ns); we estimated it to be ~ 20 ns. The sample was circulated through a Spectrasil quartz flow cell. The thickness of the flow cell varied, 0.2–10-mm path length, depending on which concentration was used. The optical density

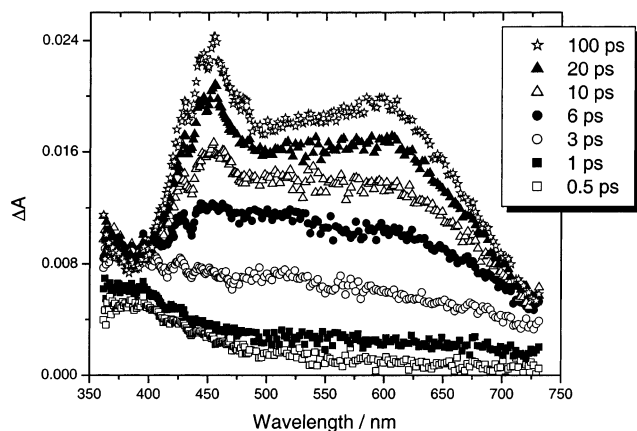


Figure 2. Transient absorption spectra of 10-mM iodoform in acetonitrile upon 350-nm excitation at various delay times between the pump pulses and probe pulses. The time delays are given in the legend in the figure.

of the sample was ~ 1 for all measurements to ensure the same number of excited molecules.

A positive transient absorption signal corresponds to an increase of absorption in both the femtosecond and the nanosecond experiments. The steady-state absorption spectra of the sample did not change during the measurement of transient absorption spectra and kinetics, ensuring no build up of photoproducts in the sample. Saturating the sample with oxygen did not affect the kinetics, ensuring that the measured signal was independent of the oxygen concentration. All measurements were performed at room temperature (21 °C) at ambient pressure. Iodoform (>98% from Fluka), cyclohexane (pa), and acetonitrile (pa) (from Merck) were used without further purification.

III. Results and Discussion

We have measured transient absorption spectra in the spectral region of 370–730 nm and kinetics at selected wavelengths on a femtosecond–microsecond time scale to explore the photodissociation dynamics of iodoform in acetonitrile and cyclohexane. Transient absorption spectra may reveal the nature of reaction intermediates and reaction products and show the temporal evolution of new species. Kinetics at specific wavelengths can give time scales of such processes as population dynamics and vibrational relaxation. A common problem in ultrafast pump–probe experiments in solution is a nonresonant coupling between pump and probe pulses in the medium (the solvent or front cell window or both), which generate signals via such mechanisms as impulsive stimulated Raman scattering (ISRS),^{15–17} induced phase modulation,^{18–20} and two-photon absorption.^{21,22} We tentatively assign the spike observed in the kinetics around time zero (± 0.3 ps) to a mixture of excited-state absorption of iodoform and a nonresonant coupling between pump and probe pulses. However, no signal from pure solvent or front cell window was observed later than ~ 0.3 ps after excitation in the entire spectral region measured. Therefore, the presented experimental results are treated as free from these signal contributions.

Figure 2 shows the measured transient absorption spectra of 10-mM iodoform in acetonitrile upon 350-nm excitation at various delay times. At early times, 0.5–1 ps after excitation, the spectra exhibit a weak absorption in the spectral region of 500–730 nm and a stronger absorption around 400 nm. The absorption grows in with time, and a broad and structureless absorption is seen in the entire spectral region after 3 ps. At

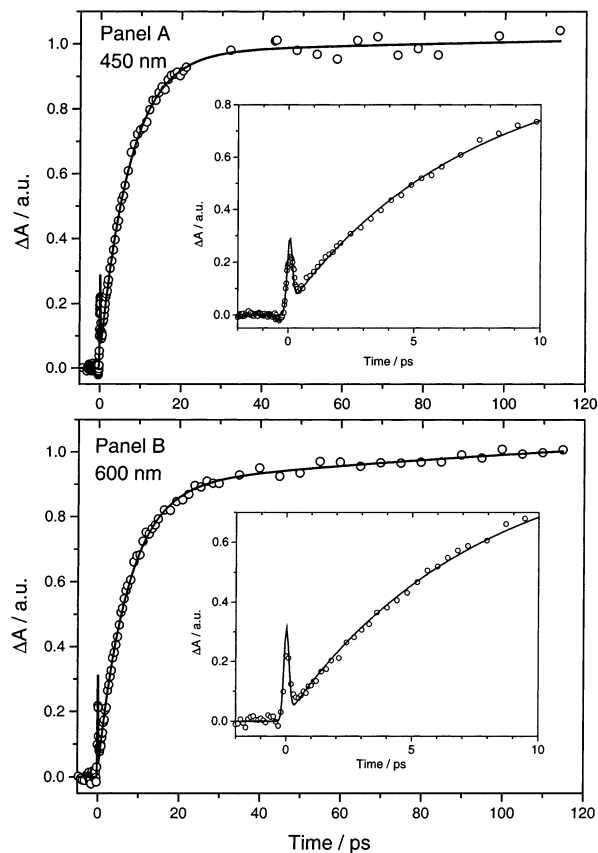


Figure 3. Normalized kinetics of 10-mM iodoform in acetonitrile following excitation at 350 nm (○), together with fits (black line). Panel A shows the kinetics at 450 nm, and panel B shows the kinetic at 600 nm. The short-time kinetics are given in the inserts.

intermediate times, 6–10 ps, the absorption is more pronounced in the region of 400–650 nm with maximum absorption around 450 nm, and an enhanced absorption around 370 nm is also observed. The spectrum sharpens into two bands after 20 ps, one strong band centered around 450 nm and another weaker and broader band centered around 600 nm. The shape of the transient absorption spectrum does not change noticeably up to 100 ps after excitation, at which time the spectrum becomes stable in the entire spectral region measured, and only minor changes in absorption intensity are observed up to 500 ps after excitation (not shown).

Normalized kinetics together with exponential fits at wavelengths within the main bands at 450 and 600 nm of the transient absorption spectrum of 10-mM iodoform in acetonitrile are shown in Figure 3. The evolution of the transient absorption signal as observed in the kinetics can be divided into three characteristic stages: a spike around time zero (± 0.3 ps) and a rise of the signal up to ~ 100 ps, followed by a more or less flat and stable signal up to 500 ps after excitation (not shown). We use the software package Spectra Solve™, version 1.5, to fit the transient absorption kinetics. An instrument response function of 230 fs (fwhm) convolutes the kinetics at time zero. The rise of the signal in the kinetics is fitted with two well-distinguished time constants, one major and fast and another minor and slow. The fast rise time of 7.2 ± 0.5 ps is identical within experimental error in the two bands, and the slower rise time is 265 ± 25 ps (see Table 2).

Which species causes the observed transient absorption? A comparison with results from photodissociation and UV-photolysis experiments of the similar dihalomethanes, CH_2I_2 , CH_2BrI , and CH_2ClI , in solution and solid matrix may be helpful

TABLE 1: The Spectral Signature of the Isodihalomethanes, CH₂I–I, CH₂Br–I, and CH₂Cl–I, Together with Those of the Photoproducts Observed in This Work and in the Work of Simon et al.²⁹

photoproduct	femtosecond work ^a			matrix isolation work by Maier et al. ^b			matrix isolation work by Simon et al. ^c		
	λ_{str} (nm) ^d	λ_{weak} (nm) ^d	I_1/I_2 ^e	λ_{str} (nm) ^d	λ_{weak} (nm) ^d	I_1/I_2 ^e	λ_{str} (nm) ^d	λ_{weak} (nm) ^d	I_1/I_2 ^e
CH ₂ Cl–I	458	723	2.3	438	745	7.6			
CH ₂ Br–I	442	632	2.7	403	660	6.0			
CH ₂ I–I/photoproduct ^f	390	560	3.3	370	545	5.9	380 ^f	530 ^f	9.0
CHI ₂ –I ^g /photoproduct ^f	450 ^g	600 ^g	1.1				445 ^f	595 ^f	2.1

^a Stable transient absorption spectra of the dihalomethanes CH₂ClI,²⁴ CH₂BrI,²³ and CH₂I₂¹¹ in acetonitrile ~50–100 ps after excitation of the low-lying state, obtained by us with the femtosecond transient absorption spectroscopy. ^b Isomer product absorption spectra of the dihalomethanes CH₂ClI, CH₂BrI, and CH₂I₂ in 12 K nitrogen matrixes after UV photolysis, performed by Maier et al.²⁵ The photoisomers CH₂Cl–I, CH₂Br–I, and CH₂I–I were identified by infrared absorption. ^c Absorption spectra of the “color centers” of CH₂I₂ and iodoform in 77 K isopentane–methylcyclohexane glass after 254-nm irradiation, performed by Simon et al.²⁷ ^d Position of the observed strong absorption maxima (λ_{str}) and the weak absorption maxima (λ_{weak}). ^e Ratio of the intensity at λ_{str} (I_1) and at λ_{weak} (I_2). ^f Simon et al.²⁷ have not assigned the observed photoproducts to the CH₂I–I or CHI₂–I isomer. ^g Observed photoproduct assigned by us to the CHI₂–I isomer.

TABLE 2: Summary of the Spectroscopic and Kinetic Observables of the Transient Absorption Spectra upon ~350-nm Excitation of Iodoform in Acetonitrile and Cyclohexane

solvent	λ (nm) ^a	τ_1 (ps) ^b	A_1 (%) ^c	τ_2 (ps) ^b	A_2 (%) ^c	$1/k$ (μ s) ^d
acetonitrile	450	7.2 ± 0.5	86	265 ± 25	14	0.22 ± 0.05
	600	7.2 ± 0.5	73	265 ± 25	27	0.23 ± 0.05
cyclohexane	450	11.0 ± 0.5	93	200 ± 30	7	1.76 ± 0.15
	600	5.1 ± 0.5	80	200 ± 30	20	1.75 ± 0.15

^a Wavelength (λ) at which the change of the transient absorption was measured. ^b Time constants from fits of the rise of the transient absorption. ^c Amplitude of the rise normalized such that $\sum A_i$ of the rise equals 100%. ^d Lifetime ($1/k$) of iso-iodoform, where k is the decay rate of the first-order process CHI₂–I → products (e.g., CHI₂ + I, CHI₃).

to identify the photoproduct. We have reported extensive femtosecond pump–probe studies of the photodissociation dynamics of the dihalomethanes CH₂I₂,¹¹ CH₂BrI,²³ and CH₂ClI²⁴ in acetonitrile. In these studies, the dihalomethanes were excited in their low-lying states and transient absorption spectra and kinetics were measured in a broad wavelength range (~290–1220 nm) up to 200–500 ps after excitation. By comparing transient absorption spectra and the photoisomer (CH₂X–I) absorption spectra measured by Maier et al.²⁵ in 12 K argon and nitrogen matrixes, we concluded that the observed photoproducts in the three studies were the isodihalomethanes. Nanosecond transient resonance Raman experiments of diiodomethane (CH₂I₂) in cyclohexane solution²⁶ confirmed this conclusion by comparing measured vibrational frequencies with those calculated by density functional theory (DFT). In addition, Simon et al.²⁷ found that 254-nm irradiation of iodoform in a 77 K isopentane–methylcyclohexane glass resulted in “color centers”, which had the same spectral features as those presently attributed to isodihalomethanes, see Table 1.

The observed stable transient absorption spectrum (>20 ps after excitation) of iodoform in acetonitrile bears a strong resemblance to the absorption spectra of the CH₂I–I,¹¹ CH₂Br–I,²³ and CH₂Cl–I²⁴ isodihalomethanes. The absorption spectra of these isodihalomethanes have the same characteristic spectral signature, two absorption bands with the strongest absorption band located at the blue side of the spectrum (see Table 1). This suggests that the observed photoproduct of iodoform is the isomer configuration of iodoform, iso-iodoform (CHI₂–I). Further support to this assignment is obtained by comparing the fast rise times of the transient absorption spectra of the isodihalomethanes CH₂I–I,¹¹ CH₂Br–I,²³ and CH₂Cl–I²⁴ in acetonitrile with the fast rise times of the iodoform photoproduct spectra in acetonitrile. The fast ~5–9 ps rise times of the

transient absorption spectra of the isodihalomethanes is mainly attributed to the formation of the dihalomethane isomers. In the same solvent, the observed fast rise time of the iodoform transient absorption spectra is ~7 ps, indicating that the observed photoproduct is of similar nature as the isodihalomethanes. DFT calculations⁹ of the iso-iodoform predict an intense ground to excited singlet state transition at 465 nm with an oscillator strength of ~0.5. This computed singlet transition energy shows a reasonably good agreement with the observed stable (greater than ~20 ps after excitation) transient absorption spectrum with an intense band at 450 nm. The computed oscillator strength for the CHI₂ radical and the CHI₃⁺ radical cation were much weaker in the spectral region of 400–470 nm.⁹ This gives additional support to our assignment. Thus, DFT calculations of excited states should be treated with care, but they can still be useful for a general exploration of electronic spectra.²⁸ Other species, such as the iodine atom (I), the CHI₂ radical, the CHI₃⁺ radical cation, and clusters of iodoform molecules, can be excluded as responsible for the observed transient absorption. Solvated iodine atoms are known to form a charge-transfer complex with acetonitrile, which has an absorption maximum at 275 nm.²⁹ DFT calculations have shown that the CHI₂ radical does not absorb above 310 nm.⁹ Direct production of the CHI₃⁺ cation can be ruled out because it requires 2.6 times more energy than the pump photon energy of ~3.54 eV used in the experiments.³⁰ Pump-energy-dependence experiments at 450 nm showed that the transient absorption signal level varied linearly upon a 4-fold reduction of the pump energy, indicating that a one-photon absorption process of iodoform induces the transient absorption changes. Steady-state absorption spectra of iodoform in acetonitrile obeyed Lambert–Beer’s law, and no change of the spectral shape was observed in the concentration range of 2–50 mM, showing that there are no preformed aggregates of iodoform in the samples used. Furthermore, the kinetics up to 500 ps after excitation at 450 nm did not change when varying the iodoform concentration in the range of 1–30 mM. Thus, clustering of iodoform molecules is not responsible for the observed strong transient absorption band.

Measured transient absorption spectra upon 350-nm excitation of 10-mM iodoform in cyclohexane as solvent are shown in Figure 4. Overall, the shape and the spectral evolution of the transient absorption spectrum of iodoform in cyclohexane are similar to those in acetonitrile. The cyclohexane transient absorption spectrum also displays a pronounced absorption around 400 nm at early times, 0.5–1 ps, and a broad and structureless absorption is observed ~3 ps after excitation. The spectrum sharpens into two bands centered around 450 and 600

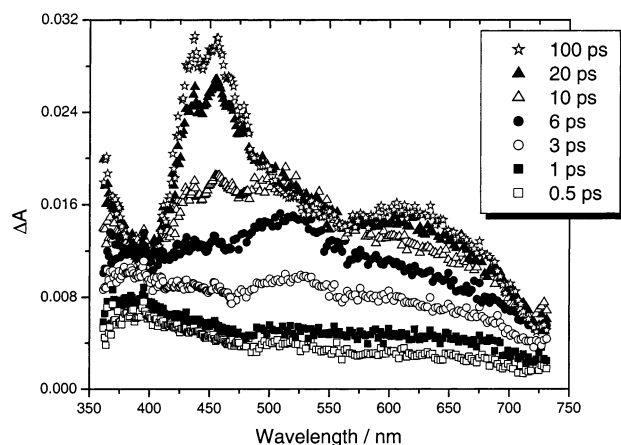


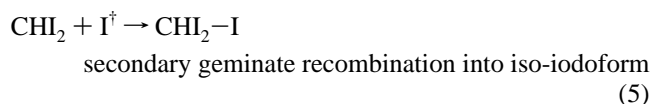
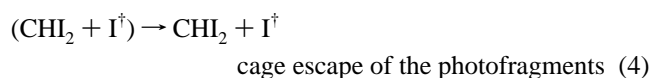
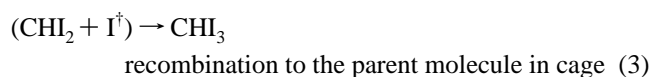
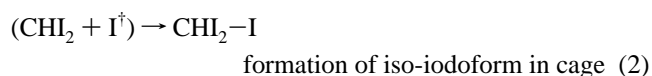
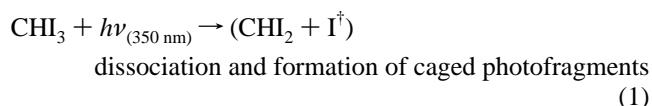
Figure 4. Transient absorption spectra of 10-mM iodoform in cyclohexane upon 350-nm excitation at various delay times between the pump pulses and probe pulses. The time delays are given in the legend in the figure.

nm together with an enhanced absorption at 370 nm at ~ 20 ps after excitation. At times 20–100 ps after excitation, the cyclohexane transient absorption spectrum sharpens further and narrows. After 100 ps, the entire transient absorption spectrum becomes stable and only minor changes in absorption intensity are observed up to 500 ps after excitation (not shown). The rise of the transient absorption signal at 450 and 600 nm in cyclohexane is also fitted with two time constants, one major and fast and another minor and slow component. The fast rise times kinetics in cyclohexane shows a somewhat different behavior compared with the one found in acetonitrile (see Table 2). However, even if the fast rise times in cyclohexane are somewhat different (see Table 2), we assign the bands to the same species, namely, the iso-iodoform, $\text{CHI}_2\text{-I}$.

The fast rise of the signal in both solvents is mainly attributed to population dynamics of the iso-iodoform, although vibrational relaxation of the hot iso-iodoform will also contribute to the dynamics. It is a well-known fact that the shape and position of transient spectra change as a result of vibrational relaxation.^{31,32} Some fraction of the iso-iodoform molecules is formed vibrationally excited after recombination of the hot photofragments. We therefore expect that the population dynamics for formation of the iso-iodoform will be accompanied by dynamics reflecting vibrational relaxation. By comparison to similar small molecules in solution,^{31,32} we expect the effects of vibrational relaxation to be most pronounced in the wings of the transient absorption spectra and thus the rise times of the centers of the bands to reflect population dynamics the best. The very broad absorption bands of the iso-iodoform even at long times after excitation will probably cause vibrational relaxation to contribute to the spectral evolution at most wavelengths. Nevertheless, the relatively small variation with wavelength of the fast rise time and limited change of spectral shape of the iso-iodoform shows that this time mainly corresponds to the formation time of the iso-iodoform.

Next we examine the transient absorption at early times. The 0.5–1 ps spectra of iodoform in both solvents exhibit a broad absorption in the 370–730 nm spectral region with a maximum absorption around 400 nm. Although DFT calculations have shown that the equilibrated CHI_2 radical does not absorb at wavelengths above ~ 310 nm,⁹ the vibrationally hot CHI_2 radical might do so, because most vibrationally hot species are expected to have a red-shifted absorption. The observed absorption around 400 nm is not likely to be due to the radical cation (CHI_3^+) because the absorption of such species are expected to occur at

different wavelengths in the two solvents with different polarities. Therefore, the observed pronounced absorption around 400 nm might be due to the absorption of the vibrationally hot CHI_2 radical. In this scenario, the following interpretation of the spectral evolution at early times can be reached. At 0.5–1 ps after excitation, the transient absorption is a mixture of the hot isomer and the hot radical. As time progresses, the hot radical relaxes and the radical absorption shifts to the blue, meanwhile the isomer absorption is growing. After ~ 3 ps, the observed broad and structureless transient absorption is mainly due to the hot iodoform isomer. At even longer times, the isomer cools and relaxes and the transient absorption spectrum sharpens and stabilizes. We propose the following reaction mechanism of the primary steps of the photodissociation of iodoform in acetonitrile and cyclohexane:



[†]where the iodine atom (I) can be in both the $\text{I}^*(^2\text{P}_{1/2})$ and $\text{I}^*(^2\text{P}_{3/2})$ states.

The majority of the iso-iodoform is most probably formed via an in-cage recombination of the hot photofragments, the CHI_2I radical and the iodine atom (see step 2), on an ~ 7 ps time scale. In acetonitrile, the observed minor and slow, ~ 265 ps, rise time (see Table 2) reflects secondary geminate recombination of cage-escaped photofragments into the iso-iodoform (see step 5). Because no spectral narrowing of the transient absorption bands is observed and vibrational relaxation is known to occur at a much faster rate (< 40 ps) in polar solvents,³³ it is not likely that vibrational relaxation contributes to the observed long rise time in acetonitrile. However, in cyclohexane, vibrational relaxation may also contribute to the observed ~ 200 ps rise time (see Table 2), because a spectral narrowing of the bands is observed and that vibrational relaxation of the parent molecule CHI_3 is known to be on a ~ 100 ps time scale in nonpolar solvents.³⁴ We have estimated the quantum yield of the formation of iso-iodoform by comparison with a 350-nm pump/probe spectra of the closely related diodomethane in acetonitrile.³⁵ Because neither the extinction coefficient of iso-iodoform is known nor any bleach is observed in the measured spectral range, we have to make the following assumptions to estimate the quantum yield. (I) Under the same experimental conditions, that is, the optical density at pump wavelength of the sample, the pump energy and the geometrical overlap was the same, excitation at 350 nm results in the same concentration of excited $\text{CH}_2\text{I}_2/\text{CHI}_3$ molecules. (II) The observed ΔA signal is only due to isomer absorption. (III) $\epsilon(\text{CH}_2\text{I-I}) = \epsilon(\text{CHI}_2\text{-I})$ or $(\epsilon(\text{CH}_2\text{I}_2)\epsilon(\text{CHI}_3)) = (\epsilon(\text{CH}_2\text{I-I})/\epsilon(\text{CHI}_2\text{-I}))$, where ϵ is the extinction coefficient at maximum absorption for the respec-

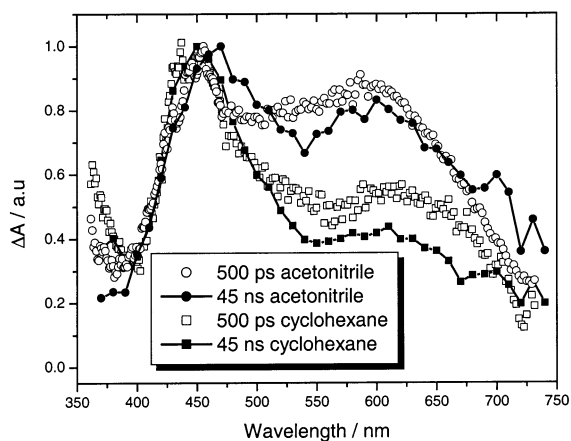


Figure 5. Normalized 45-ns transient absorption spectra upon 355-nm excitation of 10-mM iodoform in acetonitrile (—●—) and cyclohexane (—■—), together with normalized 500-ps spectra upon 350-nm excitation of 10-mM iodoform in acetonitrile (○) and cyclohexane (□).

tive molecule. By comparison of the maximum relative amplitudes in the spectra, $\Delta A(\text{CH}_2\text{I}-\text{I})/\Delta A(\text{CHI}_2-\text{I}) = (\epsilon(\text{CH}_2\text{I}-\text{I})\Phi(\text{CH}_2\text{I}-\text{I})) / (\epsilon(\text{CHI}_2-\text{I})\Phi(\text{CHI}_2-\text{I}))$, where Φ is the quantum yield of the formation of the respective isomer upon 350 nm excitation. $\Phi(\text{CHI}_2-\text{I})$ was previously calculated to be ~ 0.7 .³⁵ Then, for $\epsilon(\text{CH}_2\text{I}-\text{I}) = \epsilon(\text{CHI}_2-\text{I})$, the estimated quantum yield of the formation of iso-iodoform, $\Phi(\text{CHI}_2-\text{I})$, is ~ 0.6 in both acetonitrile and cyclohexane. This value is slightly higher than that for $(\epsilon(\text{CH}_2\text{I}_2)/\epsilon(\text{CHI}_3)) = (\epsilon(\text{CH}_2\text{I}-\text{I})/\epsilon(\text{CHI}_2-\text{I}))$, for which the $\Phi(\text{CHI}_2-\text{I})$ is ~ 0.5 and ~ 0.4 in acetonitrile and cyclohexane, respectively.

We have also performed nanosecond laser flash photolysis experiments of iodoform in acetonitrile and cyclohexane. Figure 5 shows a normalized 45-ns transient absorption spectrum upon 355-nm excitation of iodoform in acetonitrile and cyclohexane, together with a normalized 500-ps spectrum obtained by the femtosecond/picosecond experimental set up. The similarities between the nanosecond and the 500 ps transient absorption spectra in both solvents clearly show that the nanosecond transient absorption spectra are due to iso-iodoform. The nanosecond transient absorption spectra decays uniformly in both solvents, measured at 450 and 600 nm, and is fitted by a single-exponential rate constant (k_{obs}) in the concentration range of 0.2–5 mM. Also, within this concentration range, it is found that k_{obs} varies linearly with initial iodoform concentration. These observations indicate that the observed decay rate of the iso-iodoform is a sum of a first-order and a pseudo-first-order process. Thus, the observed experimental decay rate of iso-iodoform, k_{obs} , can be expressed as $k_{\text{obs}} = k + \mathcal{R}^*[\text{CHI}_3]$, where k is the rate constant of the first-order process, $\text{CHI}_2-\text{I} \rightarrow$ products (e.g., $\text{CHI}_2 + \text{I}$, CHI_3). The lifetime of iso-iodoform, $1/k \cong 1.8 \pm 0.15 \mu\text{s}$ in cyclohexane and $0.2 \pm 0.05 \mu\text{s}$ in acetonitrile, is obtained by extrapolating the linear fit of $k_{\text{obs}} = k + \mathcal{R}^*[\text{CHI}_3]$ to zero iodoform concentration at both 450 and 600 nm (see Table 2). It is evident that a nonpolar solution stabilizes the isomer. One explanation might be that the iso-iodoform can also decompose into ionic species, such as, $\text{I}^- + \text{CHI}_2^+$, in the more polar solvent acetonitrile. Because the observed absorption bands at 450 and 600 nm of the isomer decay with the same rate, it further supports our conclusion that the observed transient absorption spectra are due to absorption of one photoproduct only.

Under the same experimental conditions, the amplitude of the blue band at 450 nm at long times (> 100 ps) is the same in

the two different solvents, but the relative amplitudes of the red band around 600 nm at long times (> 100 ps) is larger and the wavelength of maximum absorption is somewhat blue-shifted in the more polar solvent acetonitrile compared to those in cyclohexane (see Figure 5). This trend, with altering relative amplitudes of the red band in different solvents is also observed for the isomer of diiodomethane, isodiiodomethane, although the effect is less pronounced.³⁶ The observed trend suggests that the ground state of the iso-iodoform is of ionic nature and that the 600-nm band is due to a charge-transfer transition. This is in agreement with the suggestion by Maier et al.³⁷ that the red band of the $\text{CH}_2\text{I}-\text{I}$, $\text{CH}_2\text{Br}-\text{I}$, and $\text{CH}_2\text{Cl}-\text{I}$ isomers has a charge-transfer character. Experimental work and advanced ab initio calculations in progress will elucidate in more detail the absorption features of the isomers.

IV. Conclusions

In this work, we have studied the photodissociation and photoproduct formation of iodoform (CHI_3) in acetonitrile and cyclohexane on an extensive time scale ranging from femtoseconds to microseconds by femtosecond pump–probe spectroscopy and nanosecond laser flash photolysis. We show transient absorption spectra in the spectral region of 370–730 nm and kinetics at selected wavelengths. The observed photoproduct with absorption maxima at 450 and 600 nm, formed upon excitation of iodoform in solution at ~ 350 nm, is assigned to the isomer of iodoform, iso-iodoform (CHI_2-I). We propose a reaction mechanism in which the majority of the iso-iodoform is formed via an in-cage recombination of the produced photofragments, the I atom and the CHI_2 radical, with an ~ 7 ps time constant. The quantum yield of the formation of the iso-iodoform was estimated to be around 0.5. The lifetime of the iso-iodoform was found to be ~ 1.8 and $0.2 \mu\text{s}$ in cyclohexane and acetonitrile, respectively.

Acknowledgment. The authors thank Dr. B. Nelander and Dr. R. Lindh for many fruitful discussions and Dr. N. Lascoux and J. Larsen for critical reading of the manuscript. Financial support from The Swedish Research Council and Magnus Bergwall Foundation is gratefully acknowledged.

References and Notes

- (1) Sato, H. *Chem. Rev.* **2001**, *101*, 2687.
- (2) Koffend, J. B.; Leone, S. R. *Chem. Phys. Lett.* **1981**, *81*, 136.
- (3) Baughcum, S. L.; Leone, S. R. *J. Chem. Phys.* **1980**, *72*, 6531.
- (4) Hunter, T. F.; Kristjansson, K. S. *Chem. Phys. Lett.* **1982**, *90*, 35.
- (5) Kawasaki, M.; Lee, S. J.; Bersohn, R. *J. Chem. Phys.* **1975**, *63*, 809.
- (6) Schmitt, G. F.; Comes, J. J. *Photochem.* **1980**, *14*, 107.
- (7) Kroger, P. M.; Demou, P. C.; Riley, S. J. *J. Chem. Phys.* **1976**, *65*, 1823.
- (8) Van den Ende, A.; Kimel, S.; Spieser, S. *Chem. Phys. Lett.* **1973**, *21*, 133.
- (9) Zheng, X.; Phillips, D. L. *Chem. Phys. Lett.* **2000**, *324*, 175.
- (10) Mohan, H.; Moorthy, P. N. *J. Chem. Soc., Perkin Trans.* **1990**, *2*, 277.
- (11) Tarnovsky, A. N.; Alvarez, J.-L.; Yartsev, A. P.; Sundström, V.; Åkesson, E. *Chem. Phys. Lett.* **1999**, *312*, 121.
- (12) Tarnovsky, A. N.; Wall, M.; Rasmusson, M.; Sundström, V.; Åkesson, E. In *Femtochemistry*; Douhal, A., Santamaria, J., Eds.; World Scientific: Singapore, 2002; p 247.
- (13) Kovalenko, S. A.; Ernstring, N. P.; Ruthmann, J. *Chem. Phys. Lett.* **1996**, *258*, 445.
- (14) Åberg, U.; Åkesson, E.; Alvarez, J.-L.; Fedchenia, I.; Sundström, V. *Chem. Phys.* **1994**, *183*, 269.
- (15) Ruhman, S.; Joly, A. G.; Nelson, K. A. *IEEE J. Quantum Electron.* **1988**, *24*, 460.
- (16) Hong, Q.; Durrant, J.; Hastings, G.; Porter, G.; Klug, D. R. *Chem. Phys. Lett.* **1993**, *202*, 183.

- (17) Kovalenko, S. A.; Dobryakov, A. L.; Ruthmann, J.; Ernsting, N. *P. Phys. Rev. A* **1999**, *59*, 2369.
- (18) Ekwall, K.; Van der Meulen, P.; Dhollande C., Berg, L.-E. *J. Appl. Phys.* **2000**, *87*, 2340.
- (19) Akhremitchev, B.; Wang, C.; Walker, G. C. *Rev. Sci. Instrum.* **1996**, *67*, 3799.
- (20) Alfano, R. R.; Ho, P. P. *IEEE J. Quantum Electron.* **1988**, *24*, 351.
- (21) Reuther, A.; Laubereau, A.; Nikogosyan, D. N. *Opt. Commun.* **1997**, *141*, 180.
- (22) Rasmusson, M.; Tarnovsky, A. N.; Åkesson, E.; Sundström, V. *Chem. Phys. Lett.* **2001**, *335*, 201.
- (23) Tarnovsky, A. N.; Wall, M.; Gustafsson, M.; Lascoux, N.; Sundström, V.; Åkesson, E. *J. Phys. Chem. A*, in press.
- (24) Tarnovsky, A. N.; Wall, M.; Rasmusson, M.; Pascher, T.; Åkesson, E. *J. Chin. Chem. Soc.* **2000**, *47*, 769.
- (25) Maier, G.; Reisenauer, H. P.; Hu, J.; Schaad, L. J.; Hess, B. A., Jr. *J. Am. Chem. Soc.* **1990**, *112*, 5117.
- (26) Zheng, X.; Phillips, D. L. *J. Phys. Chem. A* **2000**, *104*, 6880.
- (27) Simon, J. P.; Tatham, P. E. R. *J. Chem. Soc. A* **1966**, 854.
- (28) Tozer, D. J.; Amos, R. D.; Handy, N. C.; Roos, B. O.; Serrano-Andres, L. *Mol. Phys.* **1999**, *97*, 859.
- (29) Treinin, A.; Hayon, E. *Int. J. Radiat. Phys. Chem.* **1975**, *7*, 387.
- (30) Tsai, B. P.; Baer, T.; Werner, A. S.; Lin, S. F. *J. Phys. Chem.* **1975**, *79*, 570.
- (31) Owrutsky, J. C.; Raftery, D.; Hochstrasser, R. M. *Annu. Rev. Phys. Chem.* **1994**, *45*, 519.
- (32) Thomsen, C. L.; Madsen, D.; Thøgersen, J.; Byberg, J. R.; Keiding, S. R. *J. Chem. Phys.* **1999**, *111*, 703.
- (33) Elsaesser, T.; Kaiser, W. *Annu. Rev. Phys. Chem.* **1991**, *42*, 83.
- (34) Bakker, H. J. *J. Chem. Phys.* **1993**, *98*, 8496.
- (35) Tarnovsky, A. N. Unpublished data.
- (36) Tarnovsky, A. N.; Sundström, V.; Åkesson, E.; Pascher, T. Unpublished data.
- (37) Maier, G.; Reisenauer, H. P. *Angew. Chem., Int. Ed. Engl.* **1986**, *25*, 819.